



HAL
open science

Modeling of geometrical thermal distortion induced by drilling, reaming, and tapping operations

S. Han, P. Faverjon, Frédéric Valiorgue, F. Dumont, Joël Rech

► To cite this version:

S. Han, P. Faverjon, Frédéric Valiorgue, F. Dumont, Joël Rech. Modeling of geometrical thermal distortion induced by drilling, reaming, and tapping operations. 18th CIRP Conference on Modeling of Machining Operations, CMMO 2021, Jun 2021, Ljubljana, Slovenia. pp.319-324, 10.1016/j.procir.2021.09.055 . hal-04092873

HAL Id: hal-04092873

<https://hal.science/hal-04092873>

Submitted on 22 Jul 2024

HAL is a multi-disciplinary open access archive for the deposit and dissemination of scientific research documents, whether they are published or not. The documents may come from teaching and research institutions in France or abroad, or from public or private research centers.

L'archive ouverte pluridisciplinaire **HAL**, est destinée au dépôt et à la diffusion de documents scientifiques de niveau recherche, publiés ou non, émanant des établissements d'enseignement et de recherche français ou étrangers, des laboratoires publics ou privés.



Distributed under a Creative Commons Attribution - NonCommercial 4.0 International License



18th CIRP Conference on Modeling of Machining Operations

Modeling of geometrical thermal distortion induced by drilling, reaming, and tapping operations

Sangil Han^{a*}, Pierre Faverjon^b, Frédéric Valiorgue^a, Florian Dumont^a, Joël Rech^a

^aUniversité de Lyon, Ecole Centrale de Lyon - ENISE,
LTDS, UMR CNRS 5513, 58 Rue Jean Parot, 42023 Saint-Étienne, France
^bPCI SCEMM - TTGroup, Rue Copernic, 42030 Saint-Étienne, France

* Corresponding author. Tel.: +33-4-77-43-84-84; fax: +33-4-77-43-75-39. E-mail address: sangil.han@enise.fr

Abstract

This study aims at modeling the geometrical distortion induced by the heat flux generated after several drilling (D), reaming (R) and tapping operations (T). The thermal expansion over the time is estimated with the modeling of heat fluxes induced step by step during a sequence. The paper presents a method to identify heat fluxes induced into an AlSi7 aluminium workpiece during either a drilling, a reaming, or a tapping operation. These identifications have been performed with different diameters and shapes of tools using minimum quantity lubrication (MQL). A thin part having 22 holes has been manufactured by D+R+T. Its geometry has been controlled and the values have been compared with the values predicted by the model.

© 2021 The Authors. Published by ELSEVIER B.V.

This is an open access article under the CC BY-NC-ND license (<https://creativecommons.org/licenses/by-nc-nd/4.0>)

Peer-review under responsibility of the scientific committee of the 18th CIRP Conference on Modeling of Machining Operation

Keywords: Heat flux distribution; drilling; reaming; tapping; MQL; thermal distortion; machining sequence.

1. Introduction

Minimum quantity lubrication (MQL) sequence machining is widely in practice in the automobile and aerospace industries. To produce holes in the part, the MQL sequence machining process is composed of drilling (D), reaming (R), and tapping (T) [1]. Some amount of heat generated during MQL machining process can flow into the workpiece. As a result, the part is thermally expanded during MQL sequence machining, causing deviation of hole position in the part. Different tools with different geometries and diameters are adopted in the MQL sequence machining. Lots of works to identify heat flux into the workpiece during MQL/dry machining [2-6] process have been reported. As MQL is not able to remove the heat generated by cutting operations, some research works have investigated the thermal distortion of the machined part during a single MQL machining process [7][8]. Recent works have reported investigations on the thermal distortion of a more complex part having several holes by drilling sequence [9][10]. Up to now, no research papers have

studied more complex machining sequence involving several cutting processes into a complex machining sequence. Thus, this study aims at modelling the geometrical thermal distortion of a part during a MQL machining sequence (D+R+T). The case study is a gear box casing (Fig. 1) made of AlSi7 aluminium.

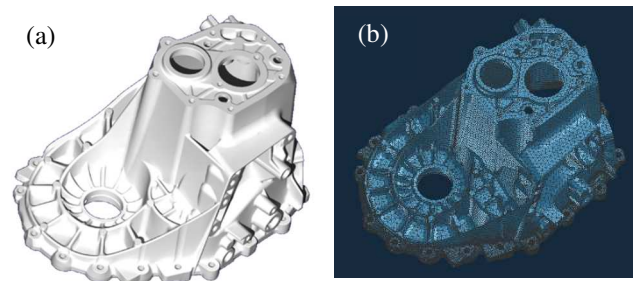


Fig. 1. (a) 3D modelling of the gear box (courtesy of PCI SCEMM); (b) its 3D mesh generation.

As a major input parameter of the modelling, heat fluxes into the workpiece during drilling, reaming, and tapping with

2212-8271 © 2021 The Authors. Published by ELSEVIER B.V.

This is an open access article under the CC BY-NC-ND license (<https://creativecommons.org/licenses/by-nc-nd/4.0>)

Peer-review under responsibility of the scientific committee of the 18th CIRP Conference on Modeling of Machining Operation

different tools are identified in the first part of this study. By means of a thermal finite element model, these heat fluxes are applied on the casing with respect to the industrial machining sequence. The thermal distortion is then simulated over the time.

Nomenclature

D	drilling
R	reaming
T	tapping
V_c	cutting speed (m/min)
f	feed (mm/rev)
d_{tool}	diameter of a tool (mm)
N	RPM (rev/min)
V_f	feed speed (mm/sec)
\dot{q}	heat flux intensity into a part (W/mm^2)
d_{th}	distance from the machined surface to the hot junction
W	work done by the process (J)
l	length of the friction zone (mm)

2. Heat flux identification in drilling, tapping, and reaming with different tools

To simulate the thermal distortion of a part due to thermal expansion during a machining sequence, it is necessary to estimate the heat flux flowing into the part during each machining operation included in the sequence. Detailed procedures to identify heat flux into the part in a single

machining (D/T/R) have been reported in the previous studies [9][10][11]. The machining sequence of the gear box casing requires several cutting tools: drills ($\phi 4$, $\phi 5.6$, $\phi 6.8$, $\phi 7.5$, $\phi 10$, $\phi 15$), reamers ($\phi 6$, $\phi 8$, $\phi 12$), and taps (M6, M8).

The heat flux distribution induced by each of them has been identified in an instrumented block made of the same alloy than the casing (AlSi7). For instance, Fig. 2 reminds the identification procedure of heat flux transmitted into the workpiece during the drilling ($\phi 10$). As shown in Fig. 2b, two heat flux distribution (W/mm^2) have to be considered in MQL drilling. The major heat source ('friction zone' in Fig. 2b) comes from the material removal and the friction on the margins close to cutting edges. The second source ('other zone' in Fig. 2b) comes from the heat of the chips. A painting deposited on the drill (Fig. 2a) enables to identify the length of the first zone, whereas the length of the second one corresponds to the length of the hole.

The intensity and shape of the heat flux distribution can be determined by fitting the calculated temperatures to the measured ones (3 replications). The maximum temperature and the residual temperature are considered to be the most important criteria to the temperature profiles fitting [5][6][9][11]. The heat flux moves at feed speed of $V_f = 40.3$ mm/sec over the hole in a finite element model in the SYSWELD[®] software (Fig. 2c). Temperatures at 3 depths (10, 30 and 40 mm) can be measured with an experimental set-up [9][10][11].

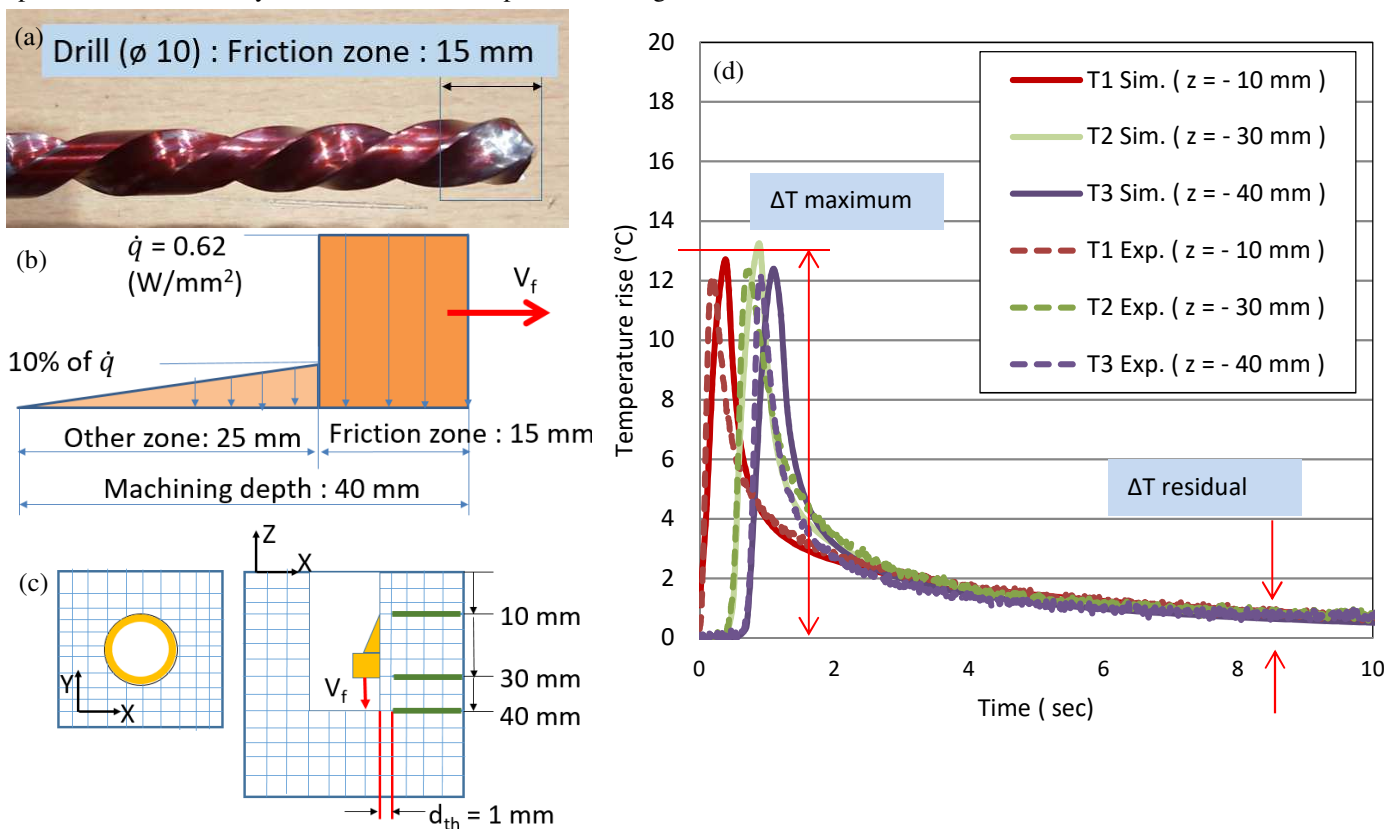


Fig. 2. Heat flux identification in drilling ($\phi 10$); (a) painted drill to reveal friction zone on margins; (b) heat flux modelling; (c) dimension of the drilled hole and heat flux application in a finite element model; (d) calculated (Sim.) and measured (Exp.) temperature profiles during MQL drilling.



Available online at www.sciencedirect.com

ScienceDirect

Procedia CIRP 00 (2019) 000–000



www.elsevier.com/locate/procedia

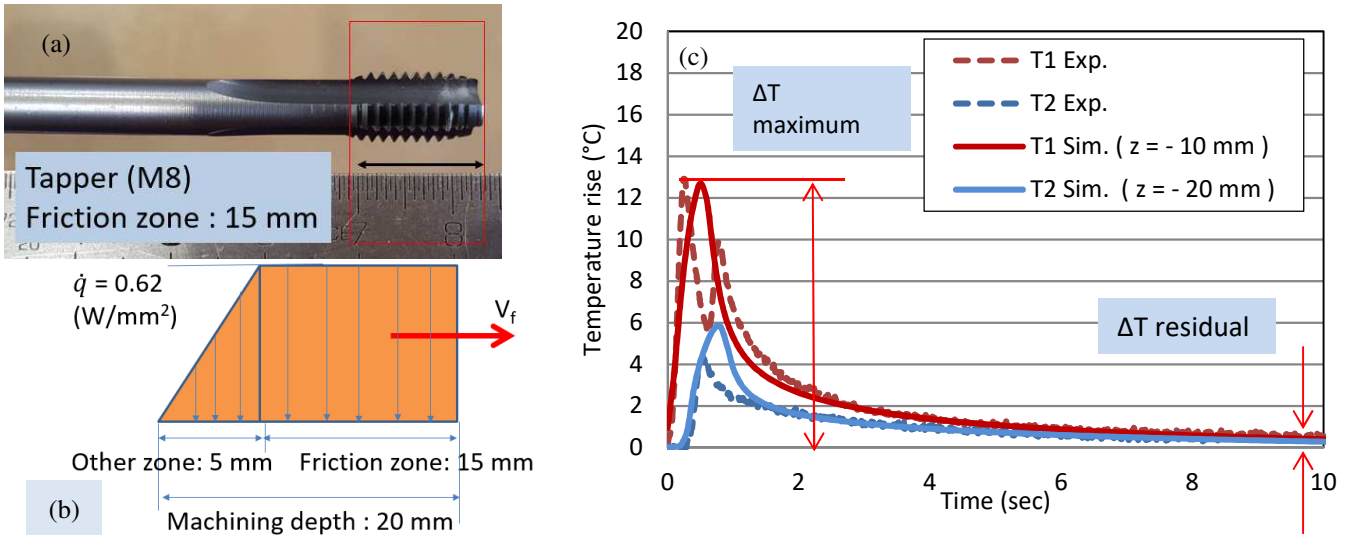


Fig. 3. Heat flux identification in tapping (M8); (a) painted drill to show friction zone; (b) heat flux modelling; (c) calculated (Sim.) and measured (Exp.) temperature profiles during tapping.

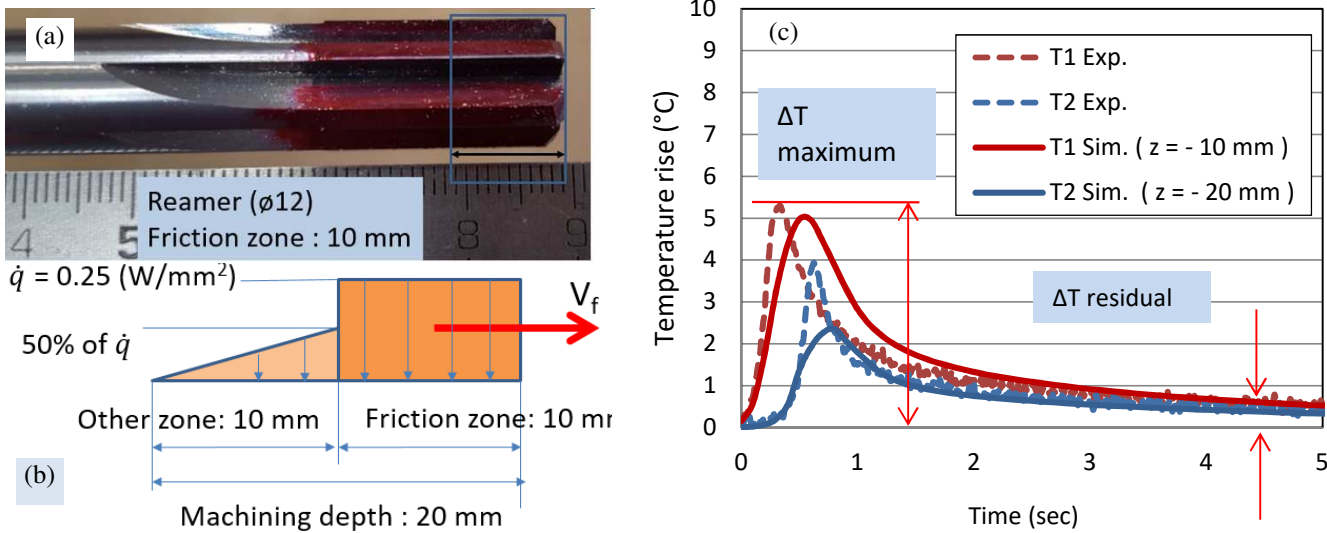


Fig. 4. Heat flux identification in reaming (ø12); (a) painted reamer to show friction zone; (b) heat flux modelling; (c) calculated (Sim.) and measured (Exp.) temperature profiles during reaming.

Table 1. The identified heat flux values and related parameters in MQL drilling, tapping, and reaming.

Process	Cutting speed, V_c (m/min)	Feed, f (mm/rev)	Tool diameter, d_{tool} (mm)	RPM, N (rev/min)	Feed speed, V_f (mm/sec)	Peak temperature rise ΔT at the hot junction (K)	The maximum heat flux density, \dot{q} (W/mm ²)	Work done by the process, W (J)
Tapping (M6x1)	40	1	6	2122	35.4	12.3	0.72	116
Tapping (M8x1.25)	40	1.25	8	1592	33.2	12.1	0.62	200
Reaming (ø6 straight)	60	0.6	6	3183	31.8	6.6	0.40	102
Reaming (ø8 straight)	100	1.2	8	3979	79.6	7.8	0.50	113
Reaming (ø12 straight)	60	1	12	1592	26.5	5.3	0.25	123
Drilling (ø15 helical)	190	0.4	15	4032	26.9	27.0	0.77	17367
Drilling (ø15 straight)	190	0.4	15	4032	26.9	39.6	1.22	10718
Drilling (ø10 helical)	190	0.4	10	6048	40.3	13.0	0.62	2355
Drilling (ø7.5 helical)	190	0.4	7.5	8064	53.8	10.8	0.62	995
Drilling (ø6.8 helical)	190	0.4	6.8	8960	59.7	10.2	0.72	618
Drilling (ø5.6 helical)	190	0.4	5.6	10800	72.0	8.7	0.62	410
Drilling (ø4 helical)	190	0.4	4	15120	100.8	7.2	0.72	95

The dimension in the experimental set-up, such as the diameter and depth of the drilled hole, depth of thermocouples embedded in the workpiece, location of the “hot junction” in the thermocouple are used in the finite element model in Fig. 2c. Detailed procedures of the finite element model are described in the studies [9][10][11]. Calculated and measured temperature profiles with respect to time are shown in Fig. 2d. Good agreement between the calculated and measured temperature profiles is shown.

A similar identification procedure has been applied for tapping. For instance, this paper presents only the case of the M8 taps in Fig. 3.

In a similar way, Fig. 4 illustrates the identification of the heat flux transmitted during the $\phi 12$ reaming operation.

The identified heat fluxes in MQL drilling ($\phi 4, \phi 5.6, \phi 6.8, \phi 7.5, \phi 10, \phi 15$), reaming ($\phi 6, \phi 8, \phi 12$), and tapping (M6, M8) were summarized in Table 1. Cutting speed (V_c), feed (f), diameter of the tool (d_{tool}), RPM (N), feed speed (V_f), and the maximum temperature rise in the workpiece (ΔT), work done by the process (W) were also given. It can be noted that temperatures were measured at thermocouple’s hot junction having a distance of $d_{th} = 1$ mm (also indicated in Fig. 2c) from the machined surface.

3. Modeling of thermal distortion in aluminum gear box during sequence MQL machining

As mentioned in introduction, the objective of this study is to model thermal distortion of the gear box casing during a complex machining sequence. A 3D CAD model of the gear box is shown in Fig. 1a. 3D meshes (type: tetra) were generated in the gear box using Visual-Mesh® as shown in Fig. 1b. As a result, 650000 elements were generated. Holes to be produced by sequence machining were assigned with a number. Their numbers were indicated in the XY and XZ views of the casing in Fig. 5. Signs C, L, and S in Fig. 5a, represent three clamping area where boundary conditions are used, a clamping point ($U_x=U_y=U_z=0$), a locating point ($U_y=U_z=0$), and a supporting point ($U_z=0$), respectively. Detailed workpiece material properties of AlSi7 and thermal boundary conditions were described in the study [10]. A convection coefficient of air of $\lambda = 4$ W/m²K was assigned to the surface of the gear box casing.

Fig. 6 presents the machining sequence. It is composed of six groups of machining operations (D+D+R+axis rotation+D+R+T). The heat fluxes were applied to each hole in accordance with the proposed machining sequence using SYSWELD®. The durations to move from one hole to another (0.1 s) have been considered in the simulation, as well as the duration to change of cutting tools (3 s), and the duration to change of orientation (rotation of axis A = 1 s). The whole machining sequence (D+D+R+axis rotation+D+T+R) requires 70 seconds. Considering cooling time of the part after machining, the deformation of the gear box was simulated during 200 seconds. The thermal distortion of the gear box casing during heat flux application is shown in Fig. 7.

The parameter U in Fig. 7 represents the normalized deformation of the part:

$$U = \sqrt{dX^2 + dY^2 + dZ^2} \tag{1}$$

where $dX, dY,$ and dZ represent displacement (mm) in the X, Y, and Z directions.

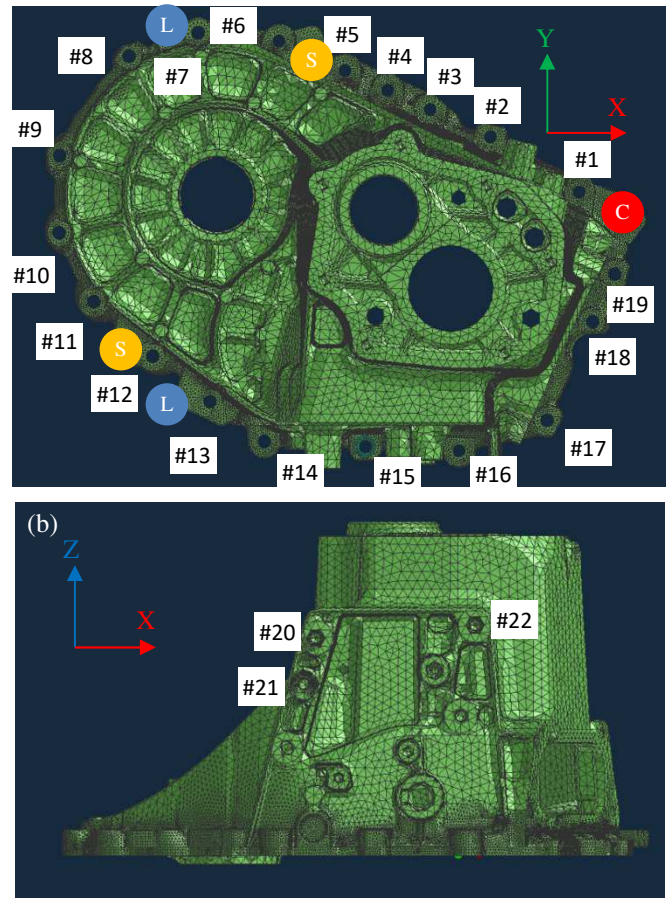


Fig. 5. Assignment of holes to be produced in the gear box: (a) the XY view; (b) the XZ view.

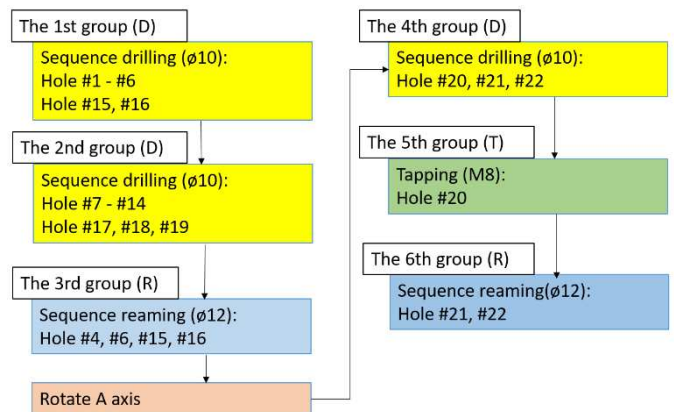


Fig. 6. Machining sequence to produce holes in the gear box.

The deformation of the gear box casing during heat flux application induces variations of the positions of the holes as compared to their theoretical location. This is one of the criteria to evaluate the accuracy of a part. A similar criteria has already been used by Faverjon et al. [9] to evaluate the displacement of holes in a drilling sequence. Therefore, Fig. 8 plots the evolution of the displacement of some holes (#1 to #19) over the time during the sequence.

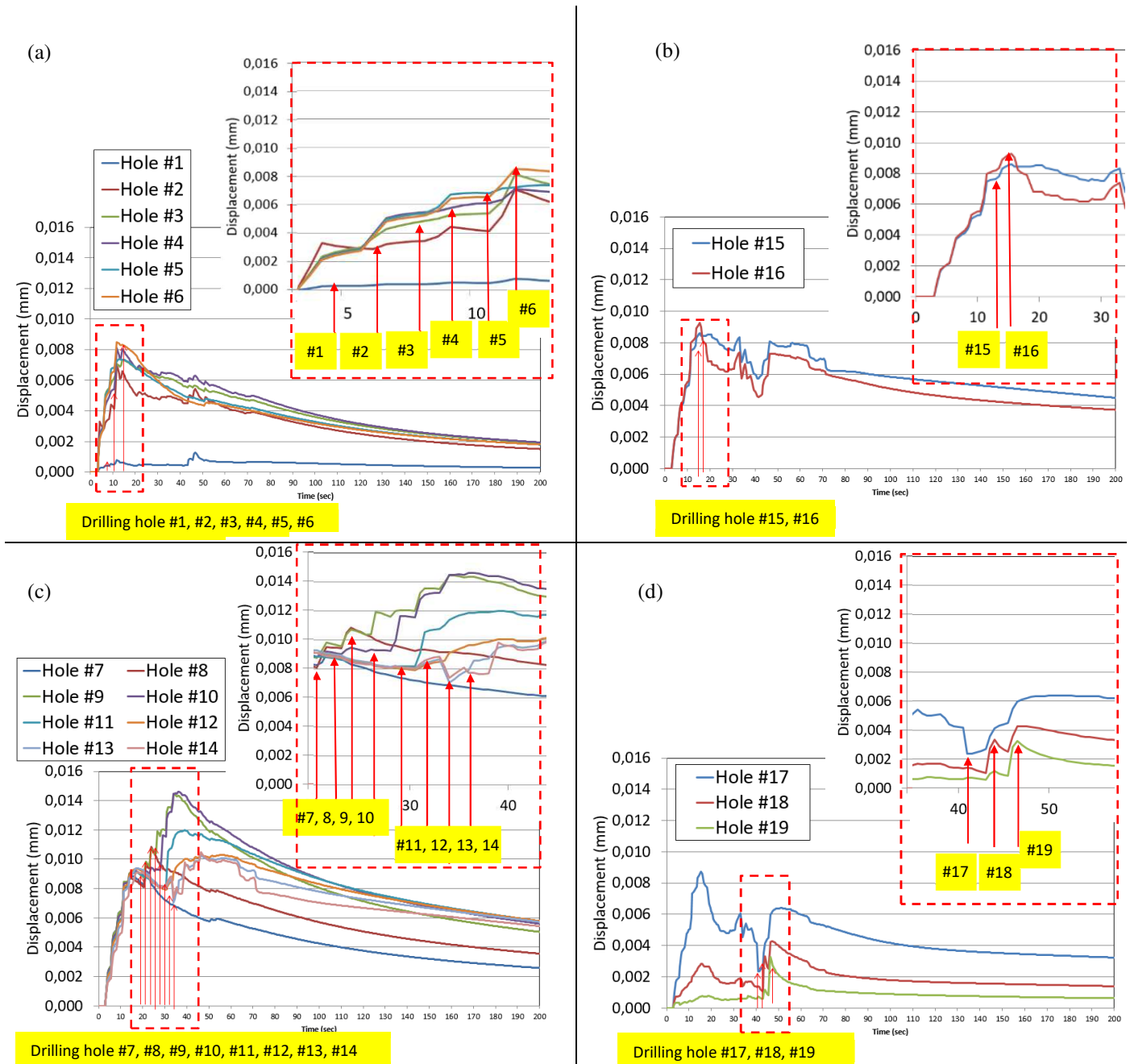
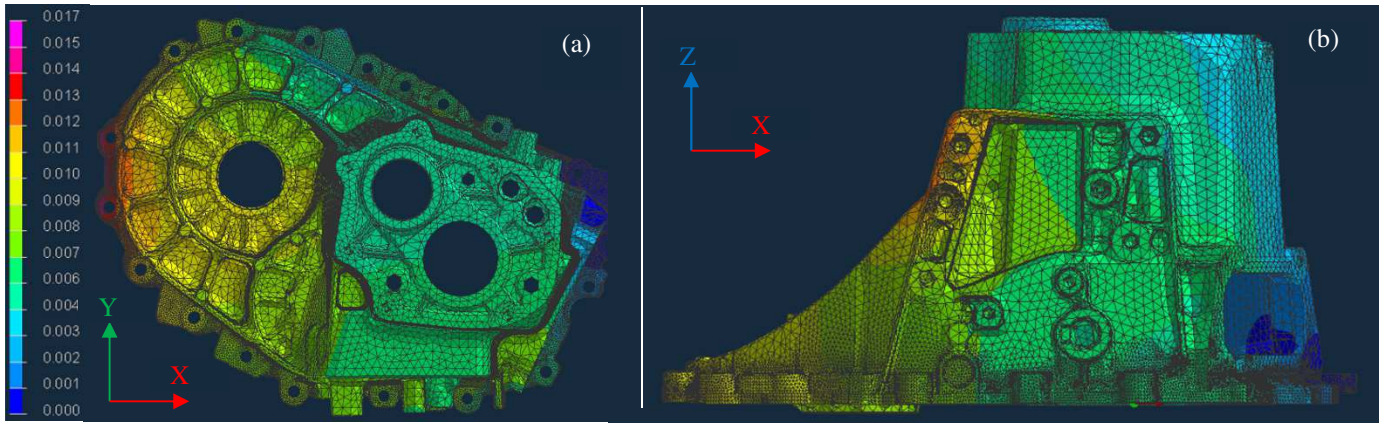


Fig. 7. Deformation of the gear box (Normalized U) in the gear box casing: (a) in the XY plane (at 40 seconds); (b) in the XZ plane (at 70 seconds). (Unit: mm)

Fig. 8. The displacements of the holes: (a) from #1 to #6; (b) #15, #16; (c) from #7 to #14; (d) #17, #18, #19 in the gear box casing.



Available online at www.sciencedirect.com

ScienceDirect

Procedia CIRP 00 (2019) 000–000



www.elsevier.com/locate/procedia

The displacement U has been quantified on 4 nodes around the hole at the middle section and averaged. On each figure, the period of each drilling operation is indicated on the time line. For instance, in Fig. 8a and b, holes from #1 to #6, and holes #15, #16 are indicated. It reveals that displacement of holes from #2 to #6 as well as holes #15, #16 increases during the first group of the drilling sequence. It was shown that, in the sequence drilling, the displacement of the hole can occur due to the thermal expansion of the other holes [10].

In Fig. 8c highlights that the maximum displacement of holes #7 to #14 do not occur during their own drilling operations. It occurs later due the heat propagation in the workpiece (macroscopic distortion of the part) and also due to the heat generated during the drilling of holes #17 to #19. A similar results has been observed by [10]. In Fig. 8d, displacement of holes #17, #18, and #19 occurs before and after their own drilling operations. This observation is also due to the thermal expansion induced by other drilling operations.

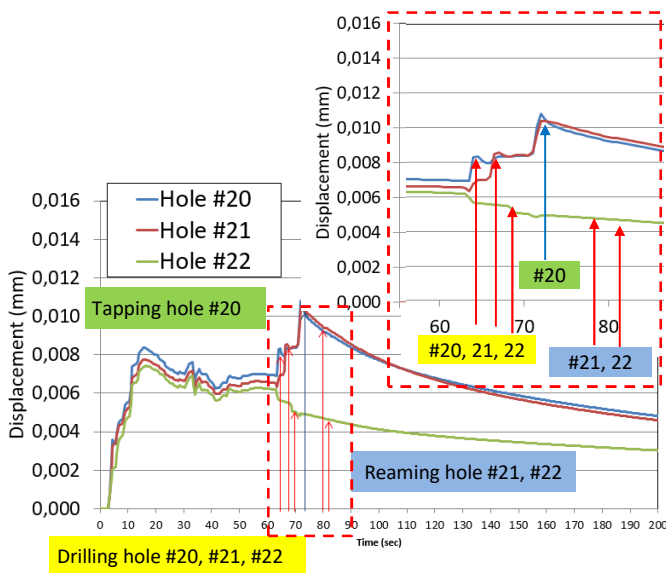


Fig. 9. The displacements of the holes #20, #21, #22 in the gear box casing for 200 seconds.

The displacements of the holes #20 to #23 are shown in Fig. 9. The maximum displacement of holes #20 and #21 occurs when the tapping of hole #20 is performed. This can be due to the heat flux generated during tapping (M8), as it is comparable to that of drilling ($\phi 10$). Moreover those two holes are close to each other. On the other hand, heat flux of reaming ($\phi 12$) is much lower than those of drilling ($\phi 10$) and tapping (M8). Thus, the reaming of holes #21 and #22 did not affect the displacement of those holes significantly.

The maximum displacement of holes occurred at hole #9 and #10 with $U = 15 \mu\text{m}$ at about 40 seconds as shown in Fig. 8c. Displacement of other holes was calculated to be less than $10 \mu\text{m}$ during sequence machining as shown in Fig. 8 and Fig. 9.

4. Discussion and Conclusion

In this study, a complex machining sequence (drilling + reaming + tapping) of 22 holes in a gear box casing has been simulated. The heat flux transmitted to the part has been quantified. It has been that the operation of drilling and tapping induces much larger amount of heat in the part. The proposed model simulates the application of the heat fluxes on each holes over the time. The displacement of each hole over the time is predicted, as well as its final position after the cooling phase. It reveals that the maximum displacement of a hole may be due either to its own drilling operation (local distortion), or to another drilling operation far from it (macroscopic distortion). The maximum deviation of the hole position was estimated to be about $15 \mu\text{m}$. This simulated result has a good agreement with the actual values observed in the industry [12]. This simulation method is shown to be effective in estimating thermal distortion of parts having complicated geometries during MQL sequence machining (D+T+R). It enables to quantify interaction between local and macroscopic distortion of complex parts over the time. The clamping conditions are considered. This modelling strategy may contribute to the optimization of a complex machining sequence. Consequently, the complex parts, such as engine block, and gear box, would gain benefits from the optimized machining sequence.

Acknowledgements

Authors thank the members of the IMPULSA project and especially to PCI and ESI Group. Authors are also grateful to H. Seux, M. Cici, P. Polly, and M. Dumas for their technical support.

References

- [1] Boyer HF, Waremme J, Bourdiol JL, Delaunay D. A study about energy consumption and cutting fluid used to clutch case machining. *Mécanique & Industries* 2011;12:389-393.
- [2] Bono M, Ni J. A model for predicting the heat flow into the workpiece in dry drilling. *Journal of manufacturing science and engineering* 2002;124:773-777.
- [3] Pabst R, Fleischer J, Michna J. Modelling of the heat input for face-milling processes. *CIRP Annals – manufacturing technology* 2010;59:121-124.
- [4] Schulze V, Pabst R, Michna J. Modeling the heat flux as an input parameter to simulate cutting processes. *11th CIRP Conference on Modelling of Machining Operations*:155-162.
- [5] Fleischer J, Pabst R, Kelemen S. Heat flow simulation for dry machining of power train castings. *Annals of the CIRP* 2007;56-1:117-122.
- [6] Boyer HF, Koppka F, Ranc N, Lorong P. Identification of the heat input during dry or MQL machining. *9th international conference on High Speed Machining* 2012;p. 1-4.
- [7] Biermann D, Iovkov I. Investigations on the thermal workpiece distortion in MQL deep hole drilling of an aluminium cast alloy. *CIRP Annals-Manufacturing Technology* 2015;64-1:85-88.
- [8] Biermann D, Blum H, Frohne J, Iovkov I, Rademacher A, Rosin K. Simulation of MQL deep hole drilling for predicting thermally induced workpiece deformations. *Procedia CIRP* 2015;31:148-153.
- [9] Faverjon P, Rech J, Valiorgue F, Orset M. Optimization of a drilling sequence under MQL to minimize the thermal distortion of a complex aluminum part. *Production Engineering* 2015;9:505-515.

- [10] Han S, Faverjon P, Valiorgue F, Rech J. Prediction and modeling of thermal distortion in sequential MQL drilling of AISi7 cylindrical parts. *Procedia CIRP* 2018;77:336-339.
- [11] Han S, Faverjon P, Valiorgue F, Rech J. Heat flux density distribution differences in four machining processes of AISi7 block: MQL drilling, tapping, reaming and dry milling. *Procedia CIRP* 2017;58:61-66.
- [12] PCI internal report, Saint Etienne in France:PCI SCEMM; 2017.